

Hamiltonian active particles in the overdamped limit

Diego M Fieguth

*State reaserch center OPTIMAS and Fachbereich Physik,
Rheinland-Pfälzische Technische Universität Kaiserslautern-Landau,
D-67663 Kaiserslautern, Germany*

(Dated: February 20, 2023)

Abstract

We examine the behaviour of a Hamiltonian particle with a degree of freedom representing an energy depot in a strongly damped environment, the so called overdamped limit. Recent papers have shown that this particular Hamiltonian mechanism, called the Hamiltonian active particle, can deplete its internal energy depot to work against external forces. We show that this behaviour persists in the overdamped limit, although it conceptually differs completely from the underdamped case. The Hamiltonian active particle adapts its behaviour to achieve the same efficiency as before. Additionally we perform a mean squared displacement analysis for a Brownian environment.

I. INTRODUCTION

Our macroscopic world is filled with energy sources that make things move. From planes to toy cars, objects have internal depots of energy that get depleted when moving against friction or other forces. In the microscopic world of biology and bio-physics, objects, such as self propelled particles [1, 2] or motile cells [3–5] for example, also move against their aqueous, frictional environment, but their inner workings are much less understood. Microscopic moving objects are often modelled by active particles with an internal energy depot[6–11]. This internal energy can displace the particle by some symmetry breaking mechanism. Every displacement in a frictional environment requires energy proportional to the velocity of the active particle. Hence, the active particle gains displacement in exchange for depot energy, that is ultimately lost as heat. In recent years active particles have gained a lot of attention but models are often phenomenological. Recent papers have shown how a minimal Hamiltonian realisation of such particles can work, with [12] and without [13] an environment. In these papers the inertial terms of the equations of motion were kept, much like in the macroscopic world. The typical regime for active particle models is however one, where inertial terms vanish. This is called the overdamped limit.

If active mechanisms have to work against large forces, they might stall completely like a car on a steep slope. But if time is no limited resource, working in regimes with comparatively high frictional forces has a simple solution: slowing down. This is due to the fact that frictional forces are proportional to the velocity, hence one has to do less work per distance at a low velocity.

In this paper we answer the question if the underdamped Hamiltonian active particle

models in [12, 13] are still able to operate in an overdamped environment. We show that instead of stalling completely, the Hamiltonian active particle automatically adjusts the timescale over which it depletes its energy depot to efficiently displace itself with the same efficiency as in the underdamped case.

A. Organisation

The paper is structured as follows. In Section II we will give a brief description of the mechanism that allows for Hamiltonian active particle (HAP) behaviour. In section III we then present the overdamped equations and show numerical solutions for two conceptually different parameter regimes. From these numerical simulations we can infer appropriate approximation methods which we apply in IV. There we apply the classical averaging theorem to the overdamped equations and a fixed point analysis. This leads to our first main result: the Hamiltonian active particle performs work as efficiently as in the underdamped case. In section V we add Brownian noise to the problem and obtain approximations to the resulting stochastic differential equation by using previous results. We give a simple expression for the mean square displacement which we compare to ensemble averages obtained by numerical realisations of the stochastic differential equation. We end with a brief conclusion in VI.

II. SETUP OF THE ACTIVE PARTICLE HAMILTONIAN

A. The Hamiltonian Model

In this section, we will briefly present the Hamiltonian model first used in [13], which was then embedded in a frictional environment in [12]. The Hamiltonian consists of two subsystems; $H_M(q, p)$ is the Hamiltonian of the particle with mass M , position q and momentum p in a linear potential (this potential is only needed to have something to do work against in the frictionless case) and $H_D(\alpha, I)$ is the Hamiltonian of the energy depot in action-angle coordinates. These two parts are weakly coupled via $\varepsilon H_C(q, \alpha, I)$ which enables the energy transfer from the depot degree of freedom to the weight. The motivation for the smallness of this coupling can be found in [13]. The small parameter ε will be important since all scales of the systems will be compared to different orders of ε . The Hamiltonians of the

subsystems and the coupling are given as

$$H_M(q, p) = \frac{p^2}{2M} + f q, \quad (1)$$

$$H_D(\alpha, I) = \omega I \quad (2)$$

$$H_C(q, \alpha, I) = -\omega \sqrt{I_0^2 - I^2} \cos(kq - \alpha). \quad (3)$$

The exposure to a frictional environment is achieved by simply adding a linear friction term $-\frac{\gamma}{M}p$ to the equation of motion for the momentum of the weight p . This leads us to the following equations for the dynamics of the system

$$\dot{q} = \frac{p}{M} \quad (4)$$

$$\dot{p} = -f - k\varepsilon\omega\sqrt{I_0^2 - I^2} \sin(kq - \alpha) - \frac{\gamma}{M}p \quad (5)$$

$$\dot{\alpha} = \omega + \varepsilon \frac{\omega I}{\sqrt{I_0^2 - I^2}} \cos(kq - \alpha) \quad (6)$$

$$\dot{I} = \varepsilon\omega\sqrt{I_0^2 - I^2} \sin(kq - \alpha) \quad (7)$$

The canonical momentum I is proportional to the depot energy ωI . Also in (7) we see that the depots values are between $-I_0 < I < I_0$.

The two typical behaviours can be seen in Figure 1. When reaching a critical speed $v_c = \omega/k$ the depot energy is either used to keep the speed from changing (blue trajectory) or the two subsystems behave as if decoupled and we observe the usual damping due to friction (dashed orange trajectory). The detailed explanation of the emergence of these qualitatively different trajectories can be found in [12] with an environment and in [13] with an external potential and without an environment. We will see later, that for the overdamped case only one kind of trajectory exists and all initial conditions with energy in the depot lead to a transfer of this energy. Hence we will not discuss these transitions. For detailed explanations of dynamical transitions and capture into a separatrix see for example [14–16]. This paper is about the overdamped limit of this specific energy transfer mechanism.

B. Non-Triviality

Energy transfer from one subsystem to another one is no rarity, so we have to emphasise how the HAP’s behaviour differs from trivial sources of energy like a compressed spring or

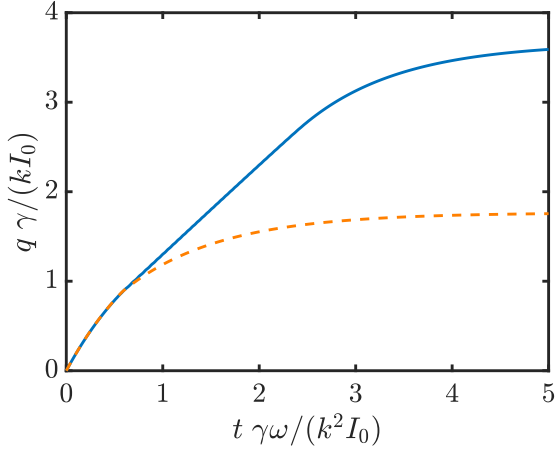


FIG. 1. Scaled position over scaled time for numerical solutions to EOM of the underdamped HAP (4)-(7), with two distinct behaviours due to different initial conditions $\alpha(0)$.

a falling weight in a potential. Both of these mechanisms can also be connected to another subsystem and transfer energy to it. The difference to the mechanism we are studying has to do with the different time scales involved. There are two important timescales for the HAP. The first one is the slow timescale, its motional degree of freedom. The second one is the fast timescale, related to its depot energy. The fast timescale was introduced in [13] as two high frequency harmonic oscillators and transformed to (1)-(3) after suitable use of adiabatic decoupling. The high frequency has the advantage that energy (proportional to frequency²) can be stored in a small volume, without using a lot of mass. For a more detailed discussion on these arguments see [13]. The slow timescale is the important one for this paper. The HAP releases its depot energy slowly and consistently to the slow motional degrees of freedom. This is even more important with friction present, since frictional forces scale with the speed of the particle. A mechanism that releases all its energy in a short amount of time, will accelerate to high speeds and use all the energy to counter high frictional forces without moving very far. A mechanism that releases its energy over a long time will operate at lower speeds, hence smaller frictional forces, and can use its energy more efficiently. We elaborate on this argument in section IV C.

C. Limitations

It is known, that for active particles to work there has to be some kind of symmetry breaking, otherwise there would not be a preferred direction of displacement. For this Hamiltonian it happens when discarding non-resonant terms in a “rotating-wave-like” approximation, shown in [13]. The “rotating-wave-like” approximation still holds if the symmetry is broken by an external force. The force thereby is not needed to assist with the transport. In our numerical simulations we disregard this external force, to better show the influence of the HAP mechanism on the displacement.

Also, we will only study how the active Hamiltonian particle uses the energy stored in its depot, we will not model energy gathering from the environment and we will always assume that we start with some energy in the depot degree of freedom. We also will not look at internal dissipation for the energy depot.

To elaborate on both of these restrictions is beyond the scope of this paper and will be subject of further publications.

III. OVERDAMPED EQUATIONS

In frictional environments, inertial terms tend to zero for a small mass. There exists an appropriate limit to the classical Langevin equation, called the overdamped Langevin equation or sometimes the Smoluchowski-Kramers approximation [17–19].

The typical manner in which we get the overdamped equations for small M is by setting $\dot{p} = 0$ to get an expression for p , which we can then insert into the equation for \dot{q} . For M to be the smallest scale in the problem, we choose $M \ll \varepsilon^2$. The overdamped equations are then calculated by setting

$$\dot{p} = 0 = -f - k\varepsilon\omega\sqrt{I_0^2 - I^2}\sin(kq - \alpha) - \frac{\gamma}{M}p \quad (8)$$

which yields

$$p = -\frac{Mf}{\gamma} - \frac{\varepsilon\omega Mk}{\gamma}\sqrt{I_0^2 - I^2}\sin(kq - \alpha) \quad (9)$$

and gives us three equations that describe the motion of the system after inserting (9)

into (4),

$$\dot{q} = -\frac{f}{\gamma} - \frac{\varepsilon k \omega}{\gamma} \sqrt{I_0^2 - I^2} \sin(kq - \alpha), \quad (10)$$

$$\dot{\alpha} = \omega + \varepsilon \frac{\omega I}{\sqrt{I_0^2 - I^2}} \cos(kq - \alpha), \quad (11)$$

$$\dot{I} = \varepsilon \omega \sqrt{I_0^2 - I^2} \sin(kq - \alpha). \quad (12)$$

Since all expressions only depend on the difference of $kq - \alpha$ we can combine the first two equations into one equation for $\varphi := \alpha - kq$,

$$\dot{\varphi} = \omega + \frac{kf}{\gamma} + \varepsilon \omega \left(\frac{I}{\sqrt{I_0^2 - I^2}} \cos(\varphi) - \frac{k^2}{\gamma} \sqrt{I_0^2 - I^2} \sin(\varphi) \right) \quad (13)$$

which results in the depot energy obeying

$$\dot{I} = -\varepsilon \omega \sqrt{I_0^2 - I^2} \sin(\varphi). \quad (14)$$

The time evolution of I obtained by numerical integration of (13),(14) can be seen as the orange line in Figure 2 for illustrative parameters. The black line is the averaged solution discussed in Section IV. We can clearly see that the depot is depleting, from which we expect movement since energy can only be lost to friction. The simple dependence of q on the depot energy can be seen in (10) in the following way: Noticing that the second term is just $-\frac{k}{\gamma} \dot{I}$, we can integrate (10) which gives us

$$q(t) = q(0) - \frac{f}{\gamma} t - \frac{k}{\gamma} (I(t) - I(0)). \quad (15)$$

This confirms that decreasing I means increasing q .

In Figure 2 we can see numerical solutions of the overdamped equations for the HAP in two parameter regimes. In Figure 2 a) we can see small oscillations due to the so called fast rotating phase φ . For problems involving such a fast angle φ we can average the evolution for I . The averaged evolution is sufficient since (15) translates the depleted depot energy to displacement. In Figure 2 b) we show a regime where the depot energy depletes linearly, without oscillations. These two regimes will be investigated in the next section.

IV. ANALYTIC DESCRIPTION OF THE BEHAVIOUR

In the last section we derived the overdamped equations of the Hamiltonian system from Section II. We reduced the set of equations of motion to two, namely the coordinates (φ, I) .

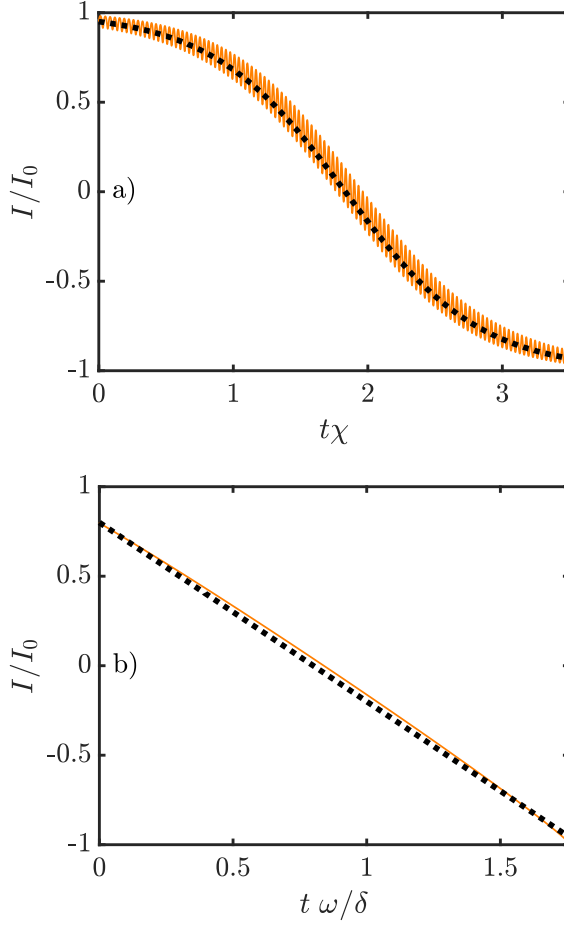


FIG. 2. In a): Solution of rescaled I over rescaled time, gained by numerically integrating (13),(14) (solid orange line) with initial conditions $\varphi(0) = -\pi/2, I(0) = 0.95$. In a) we can also see the averaged solution (22) for $I(0) = 0.95$ (thick black line) for $\omega = k = \gamma = M = 1, f = 0$ and $\varepsilon = 0.1$. The parameter χ is defined in (23). These parameters were chosen to be illustrative and show the effect of the different timescales. In b): Solution of rescaled I over rescaled time, gained by numerically integrating (13),(14) (solid orange line) with initial conditions $\varphi(0) = 2, I(0) = 0.8$. In b) we can also see the approximative solution (25) for $I(0) = 0.8$ (dashed black line) for $\omega = \gamma = M = 1, f = 0, k = 25$ and $\varepsilon = 0.1$. The parameter δ is defined in (20).

So the full dynamics of the system will be described by these two variables. The quantity we are interested in however is the position q . We want to know how far the HAP will move in the frictional environment. This highlights the importance of (15), which relates q and I . This means any analytical approximation of the depot variable I will give us an approximation of the displacement.

Here we will make suitable approximations in two complementary parameter regimes shown in Figure 2.

First we find a simplified (averaged) description of the dynamics in the (φ, I) -system, yielding a simple time evolution for I , which we then can use to figure out the displacement using (15). In the derivation of the averaged description we rely on a certain parameter to be small. The case where this parameter is large is investigated separately at a later point in this section.

A. Application of the averaging Theorem

Here we will use standard averaging arguments due to the fact that ω is the fastest time scale in the system. From the time evolution in Figure 2 a) we see that before I is changing significantly there are many small oscillations resulting from the fast evolution of φ . We will now average the equation for I , obtaining an average value \bar{I} , and derive an expression for the thick black line in Figure 2 using the fact that ε is small. For brevity we will also assume that the external force is $f = 0$. We first look at the integral of \dot{I} over a short time $\Delta t \gg \omega^{-1}$

$$\Delta I = \int_0^{\Delta t} dt \dot{I} = \int_0^{\Delta \varphi} d\varphi \frac{\dot{I}}{\dot{\varphi}}. \quad (16)$$

Since I changes on a much slower scale than φ , we can approximate the integral by

$$\Delta I \approx \frac{\omega \Delta t}{2\pi} \int_0^{2\pi} d\varphi \frac{\dot{I}}{\dot{\varphi}}. \quad (17)$$

Colloquially speaking, the prefactor in (17) determines how often the integral in (17) fits into the integral expression in (16). Also \dot{I} and $\dot{\varphi}$ should be understood as functions of φ and the current average value \bar{I} . Inserting (13) and (14), we are now left with the coarse grained change of I given by

$$\dot{\bar{I}} := \frac{\Delta I}{\Delta t} = -\frac{\varepsilon \omega}{2\pi} \sqrt{I_0^2 - \bar{I}^2} \int_0^{2\pi} d\varphi \sin(\varphi) \left(1 + \varepsilon \left(\frac{\bar{I}}{\sqrt{I_0^2 - \bar{I}^2}} \cos(\varphi) - \frac{k^2}{\gamma} \sqrt{I_0^2 - \bar{I}^2} \sin(\varphi) \right) \right)^{-1}. \quad (18)$$

It is easy to see that the zeroth order in ε of the integrand vanishes since we integrate

$\sin(\varphi)$ over one period. The first order Taylor expansion of the integrand in(18) yields

$$-\int_0^{2\pi} d\varphi \sin(\varphi) \left(\frac{\bar{I}}{\sqrt{I_0^2 - \bar{I}^2}} \cos(\varphi) - \frac{k^2}{\gamma} \sqrt{I_0^2 - \bar{I}^2} \sin(\varphi) \right), \quad (19)$$

which is a viable approximation as long as

$$\delta := \frac{k^2 I_0}{\gamma} \ll \frac{1}{\varepsilon} \quad (20)$$

holds. The case of large δ will be considered separately.

The product $\sin(\varphi) \cos(\varphi)$ also vanishes after integrating and we are left with a non-vanishing integral over $\sin^2 \varphi$. This leads us to the averaged evolution

$$\dot{\bar{I}} = -\frac{\varepsilon^2 k^2 \omega}{2\gamma} (I_0^2 - \bar{I}^2) + \mathcal{O}(\varepsilon^3) \quad (21)$$

which has the simple solution

$$\bar{I}(t) = -I_0 \tanh(\chi(t - t_0)), \quad (22)$$

where

$$\chi = \frac{\varepsilon^2 k^2 \omega I_0}{2\gamma} \quad (23)$$

and $t_0 = \chi^{-1} \operatorname{arctanh}(\bar{I}(0)/I_0)$. The averaged solution (22) can be seen in Figure 2 as the thick black line. Even though the numerical evolution was done for a rather large $\varepsilon = 0.1$, the averaged solution describes the secular depletion of the depot energy well as long as δ is not too large (see (20)).

B. Fixed point analysis

The HAP enters a qualitatively different regime when (20) does not hold. There is a critical value for which φ has a fixed point, namely if

$$\sin(\varphi^*) = \frac{\omega}{\delta \varepsilon} \quad (24)$$

has a real solution. If the value of I is not too close to the extremal values $\pm I_0$, we can neglect the first order of ε in (13),(14) to get a stationary phase value $\dot{\varphi} = 0$ around $I = 0$.

If this happens the depot energy changes like $\dot{I} = -I_0 \omega / \delta$ with an error of order $\varepsilon \omega \sqrt{I_0^2 - \bar{I}^2}$. With $I(0) = 0$ leads to the solution

$$I^{(0)}(t) = -I_0 \frac{\omega}{\delta} t \quad (25)$$

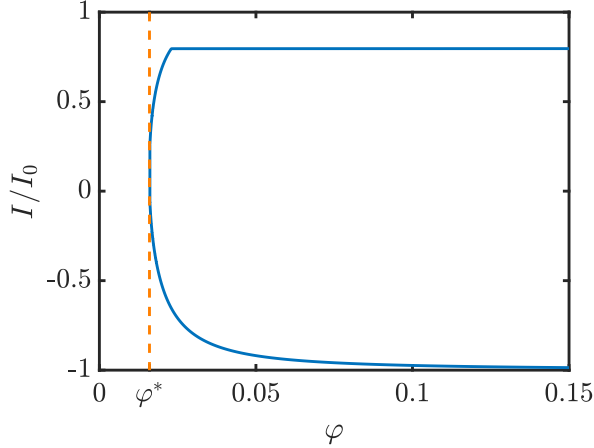


FIG. 3. Numerical solution to (10)-(12). The trajectory in phase space (blue) can be seen with the limiting value φ^* (dashed orange). This is the corresponding phase space evolution to Figure 2 b).

in zeroth order in ε . This zeroth order solution can be seen as the dashed black line in Figure 2 b). The deviation in Figure 2 b) can be explained by looking at higher orders. The first order in ε , $I^{(1)}$, for example can be obtained by inserting the zeroth order solutions ($\varphi^{(0)} = \varphi^*$, $I^{(0)}$) into the equation of motion,

$$\dot{I}^{(1)} = -\varepsilon\omega\sqrt{I_0^2 - I^{(0)}(t)^2}\sin(\varphi^*) = -\varepsilon I_0\omega\sqrt{1 - \frac{\omega^2}{\delta^2}t^2}. \quad (26)$$

The behaviour of the phase φ in this regime can be seen in Figure 3. The trajectory of the numerical solutions is shown in the (φ, I) -phase-space in blue. We clearly see that it approaches the value $\varphi^* = \arcsin(\omega/(\varepsilon\delta))$ around $I = 0$. Near this fixed value, the depot energy changes. The time evolution of the depot energy corresponding to Figure 3 was already shown in Figure 2 b). There we can confirm the depleting depot energy, which in return means increasing position $q(t)$ (see (15)).

This means we can confirm the depleting depot in two opposing regimes.

Now that we know the scales involved in the evolution of the energy in the depot for different parameter regimes, we can discuss the efficiency.

C. Efficiency

We will now compare the HAP to an instantaneous energy transfer and examine how far the particle can move. A particle in a frictional environment will follow the equation of

motion

$$\dot{q} = -\frac{\gamma}{M}q, \quad (27)$$

which has the solution

$$q(t) = L \exp\left(-\frac{\gamma}{M}t\right), \quad (28)$$

where L is the distance travelled against friction. The initial energy is the kinetic energy since no potentials are involved,

$$E_0 = \frac{M}{2}\dot{q}(0)^2 = \frac{M}{2}\left(\frac{L\gamma}{M}\right)^2 = \frac{L^2\gamma}{2M}. \quad (29)$$

The displacement in dependence of the input energy is then

$$L(E_0) = \sqrt{\frac{2ME_0}{\gamma^2}}. \quad (30)$$

We see that the distance travelled just vanishes in the overdamped limit $M \rightarrow 0$.

1. Efficiency in the small δ regime

For the HAP we have an initial energy of order ωI_0 in the depot and a kinetic energy of

$$E_{\text{kin}} = \frac{M}{2}\left(\frac{k\chi}{\gamma I_0}(I_0^2 - I(0)^2)\right)^2, \quad (31)$$

which vanishes for $M \rightarrow 0$. If we choose $M = \mathcal{O}(\varepsilon^z)$ with $z > 2$, M is still the smallest scale, smaller than $\chi = \mathcal{O}(\varepsilon^2)$. This justifies the overdamped limit and we have the energy

$$E_0 = I_0\omega + E_{\text{kin}} = I_0\omega + \mathcal{O}(\varepsilon^{4+z}). \quad (32)$$

The displacement L_{HAP} for the HAP can be identified from (10) to be of order

$$L_{\text{HAP}} = \frac{kI_0}{\gamma} = \frac{kE_0}{\omega\gamma} + \mathcal{O}(\varepsilon^{4+z}). \quad (33)$$

Comparing the displacements (30) and (33), we see that the Hamiltonian mechanism is far more effective in using the initial energy E_0 to gain displacement since the distance is not effected by the mass M .

The HAP in this regime acts like an efficient car driver: it maximises the travelled distance by slowing down and using the fuel (depot energy) against smaller frictional forces.

The HAP is however not as effective as it could be, in fact it has the same effectiveness as its underdamped version from Section II. In the underdamped case the travel speed is $v_c = \omega/k$, which results in an average frictional force of magnitude γv_c . With the same available depot energy E_0 we get the same equation (33) for the underdamped case.

While the overdamped HAP does only have a maximum speed of order ε (see (10)), most of the motion is just back and forth. This can be seen as the small oscillation in Figure 2. This figure shows the depot energy, which is directly proportional to (15). Without this non-secular motion, speeds of order ε would result in an efficiency of order ε^{-1} over timescales of the same order. The back and forth during one cycle of φ causes the HAP to generate secular displacement over a much longer time scale of ε^{-2} , hence ending up with the same efficiency as in the underdamped case.

2. Efficiency in the large δ regime

For large values of the parameter δ we need to reevaluate the efficiency. In contrast to the small δ regime, I does not show small oscillations. This is attributed to the phase φ barely changing during the entire evolution.

Using the zeroth order approximation of I from equation (25) the velocity is

$$\dot{q} = -\frac{k}{\gamma} \dot{I} = \frac{k^2}{k\gamma} \frac{I_0 \omega}{\delta} = \frac{\omega}{k}. \quad (34)$$

We recover the critical speed from the underdamped HAP $v_c = \omega/k$. This means the efficiency stays the same for the underdamped case and the overdamped cases with small and large δ . For large δ the HAP moves faster and experiences higher frictional forces, but secular displacement also appears in the zeroth order in ε .

V. BROWNIAN ENVIRONMENT

In this section we add Brownian noise with a strength that allows for the active transport to be observed. For this we specify how the noise scales with ε .

A. Scales of the Brownian noise

Before discussing the HAP in a Brownian environment, we have to identify the appropriate scales of Brownian noise, for which we will assume white noise. The Brownian motion has a variance given by the Einstein relation $\sigma^2/2 = \gamma k_{\text{B}} T$ [20]. The easiest case is the decoupling case, where the evolution of φ, I is unchanged in the first non-vanishing order in ε .

For the small δ regime, the Brownian noise has to be of second order in ε in order to be negligible in the evolution of φ, I . This coincides with the case where the speed due to diffusion is on the same order as the averaged velocity of the HAP which is of order $\chi = \mathcal{O}(\varepsilon^2)$. This means the Brownian noise scales like

$$\sigma^2 = \mathcal{O}(\chi) = \mathcal{O}(\varepsilon^2) \quad (35)$$

in the dimensionless parameter ε . Larger noise will dominate all influence of the active mechanism.

For the case of large δ the decoupling intensity is of lower order, so

$$\sigma^2 = \mathcal{O}(\varepsilon). \quad (36)$$

The case where the speed due to diffusion is of the same order as the active mechanism is the case where the noise is of order ε^0 .

B. Motion with Brownian Noise

We look at same equations but add a white noise term to the position

$$\dot{q} = -\frac{f}{\gamma} - \frac{\varepsilon \omega k}{\gamma} \sqrt{I_0^2 - I^2} \sin(kq - \alpha) + \dot{W}_t = \frac{f}{\gamma} - \frac{k}{\gamma} \dot{I} + \sigma \dot{W}_t \quad (37)$$

where \dot{W}_t is to be interpreted as the Wiener process in the sense of distributions. The standard deviation should be of appropriate order in ε , like discussed in the previous subsection. The effect of the noise term in \bar{I} can be neglected since it is of order a higher order in ε in expansion (19).

For a vanishing force f , and $\sigma = \mathcal{O}(\varepsilon^2)$ it holds that

$$q(t) = q(0) + \frac{k}{\gamma} I(0) + \frac{k}{\gamma} \tanh(\chi(t - t_0)) + \sigma W_t + \mathcal{O}(\varepsilon^3). \quad (38)$$

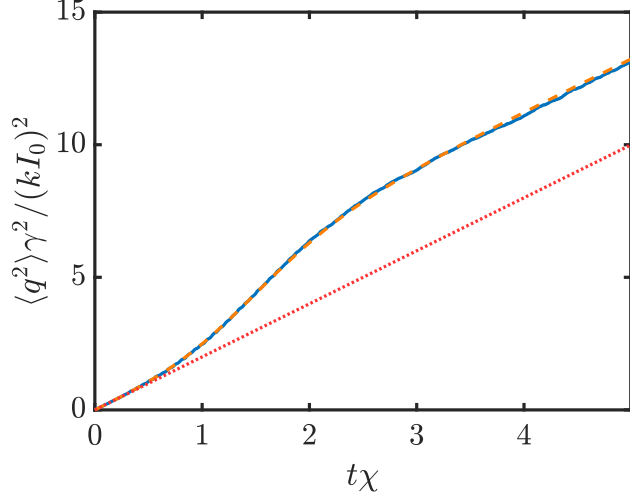


FIG. 4. The (scaled) mean squared displacement of 10^4 sample trajectories (blue) obtained by solving (10)-(12) with additional white noise in (10) plotted over (scaled) time. The dashed orange corresponds to the analytical result of result of (42). The red dotted line depicts the diffusive term $\sigma^2 t$. The numerical integration was performed for $\omega = \sigma \varepsilon^{-2} = \gamma = k = I_0 = 1$, $f = 0$ and $\varepsilon = 0.01$ with initial conditions $I(0) = 0.8$, $q(0) = 0$, $\alpha(0) = -\pi/2$.

Keeping only the lowest orders of ε , this leads to a mean square displacement behaving like

$$\langle q^2 \rangle(t) = \left\langle \left[q(0) + \frac{k}{\gamma} I(0) + \frac{k}{\gamma} \tanh(\chi(t - t_0)) + \sigma W_t \right]^2 \right\rangle, \quad (39)$$

$$= \left[q(0) + \frac{k}{\gamma} I(0) + \frac{k}{\gamma} \tanh(\chi(t - t_0)) \right]^2 \quad (40)$$

$$+ 2\sigma \left[q(0) + \frac{k}{\gamma} I(0) + \frac{k}{\gamma} \tanh(\chi(t - t_0)) \right] \langle W_t \rangle + \sigma^2 \langle W_t^2 \rangle, \quad (41)$$

$$= \left[q(0) + \frac{k}{\gamma} I(0) + \frac{k}{\gamma} \tanh(\chi(t - t_0)) \right]^2 + \sigma^2 t. \quad (42)$$

This analytical result can be seen in Figure 4 as the dashed orange line. The blue line is the mean square displacement over numerically simulated trajectories of the HAP in a Brownian environment. The dotted red trajectory shows the mean square displacement in absence of the energy depot. We see that on top of the diffusion there is a clear displacement that has its origins in the conversion of the depot energy we have seen in the previous section. When the depot is nearly depleted the mean squared displacement continues to grow with the diffusive growth constant.

For small values of δ the case where effects of HAP and effects of diffusion were of the same order coincided with the case of noise decoupling from the depot degree of freedom in the lowest non-vanishing orders. This is no longer the case in the regime of large δ as was described in Section V A.

The easiest case we can assume is the decoupling of the noise from φ . This is the case if $k\sigma\dot{W}_t$ is of order one or higher in ε in (13). An easy choice is i.e. $k\sigma = \mathcal{O}(\sqrt{\varepsilon})$ so the noise is of order ε . This means the large δ case also allows for larger noise than the small δ case, without effecting the depot energy degree of freedom. The small δ case explained above required the noise to be at least of order ε^2 , to have comparable effects on the time the energy depot takes to drain.

In the decoupling regime however, the influence of the Brownian noise is small compared to the displacement generated by the HAP. Over a time interval such that $t\omega/\delta = \mathcal{O}(1)$ the mean squared displacement originating in the diffusion is of order ε . This decoupling case can be seen in Figure 5 a). The HAP exerts a force inducing a constant velocity (see Section IV B) resulting in a parabolic trajectory in the squared displacement plot. The corresponding depot energy can be seen in 5 b), and a comparison to Figure 5 a) shows that the parabolic behaviour persists as long as the HAP drains its depot energy.

If we assume comparable noise of order v_c , the stochastic analysis in the (φ, I) -space becomes more complicated. We will omit the exhaustive analysis, since there is very little to gain from it. In the presence of fixed points in φ , trajectories spend a transient time in their vicinity, before looping around to $\varphi^* \pm 2\pi$ and repeating the same process. The onset of this effect can be seen in Figure 5 c), where transient times are spent near $\varphi^* + 2\pi n$.

VI. CONCLUSION

Over the course of this paper we have shown how an active Hamiltonian particle converts its internal energy in the overdamped limit. The surprising result is that the Hamiltonian active particle has the same efficiency as in the underdamped case. This happens in two opposing parameter regimes, with completely different dynamics.

In section II we briefly reviewed the HAP and its key features, including the down-conversion from high frequency degrees of freedom to low frequency degrees of freedom over a long time scale. In section III we derived the overdamped equations from the four initial

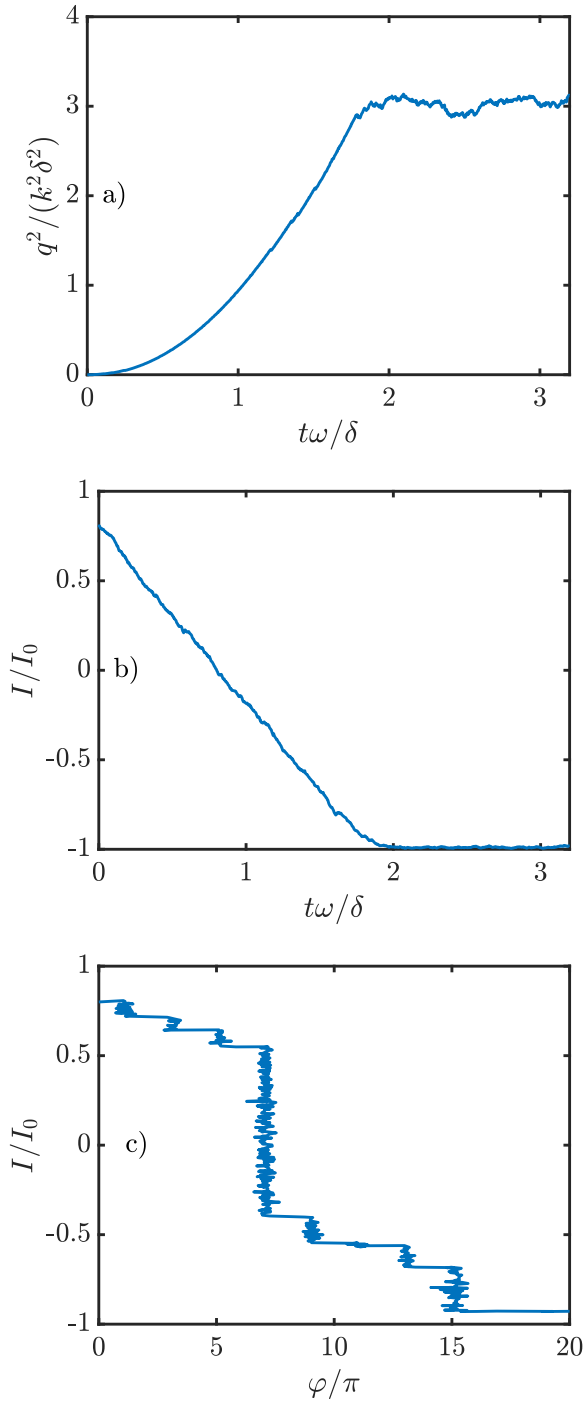


FIG. 5. Numerical solution to (10)-(12) with added noise $\varepsilon \sigma \dot{W}_t$ in (10). In a) we see the time evolution of the position. In b) the time evolution of the depot energy is depicted (blue). In c) the trajectory in the (φ, I) -space is shown. The numerical integration was performed for $\omega = \gamma = I_0 = 1$, $f = 0$, $k = 25$ and $\varepsilon = 0.01$. To best show the transient effects we chose $\sigma/\sqrt{\varepsilon} = 0.7$.

equations and further reduced the number of equations to two. We presented a numerical integration of the overdamped equations of motion, which showed emptying of the depot degree of freedom for two completely different dynamical regimes. Both of the regimes resulted in a displacement of the Hamiltonian active particle.

In section IV we analysed the two opposing parameter regimes. In the first regime we showed by using the averaging theorem and an expansion in a small parameter that the mean change of the depot energy follows a simple solvable differential equation. In the second regime we built our analysis around fixed points in the phase. There we showed that the energy depot drains linearly and results in the same critical speed known from the underdamped equations.

We compared the two overdamped evolutions to an instantaneous energy transfer. We showed that the displacement generated by the Hamiltonian active particle is finite, even in the overdamped limit. For the instantaneous energy transfer, the displacement vanished in the overdamped limit. In section V we built on the analytic approximations and discussed the mean squared displacement analysis for appropriate noise intensities in both of the regimes.

The main result of this paper is, that the Hamiltonian active particle does work in an overdamped environment. It does not only function but it does so with the same efficiency as in the underdamped case. And that is only when looking at trajectories that allow an energy exchange. We have to keep in mind that only a fraction of trajectories show an energy exchange in the underdamped case. This gets usually expressed as a probability (since initial conditions that show either behaviour are strongly mixed) that is of order $\sqrt{\varepsilon}$. This means the Hamiltonian active particle is actually *more efficient* in an overdamped environment. Not because the energy is used more efficiently, but because almost every initial condition exchanges energy, independent of ε .

The Hamiltonian active particle does not simply survive the exposure to an overdamped environment, it flourishes in it.

ACKNOWLEDGMENTS

The author thanks James R. Anglin for the valuable discussion on the topic and acknowledges the support from State Research Center OPTIMAS and the Deutsche Forschungsge-

meinschaft (DFG) through SFB/TR185 (OSCAR), Project No. 277625399.

- [1] J. R. Howse, R. A. Jones, A. J. Ryan, T. Gough, R. Vafabakhsh, and R. Golestanian, Self-motile colloidal particles: From directed propulsion to random walk, *Physical Review Letters* **99**, 10.1103/PhysRevLett.99.048102 (2007).
- [2] W. F. Paxton, K. C. Kistler, C. C. Olmeda, A. Sen, S. K. S. Angelo, Y. Cao, T. E. Mallouk, P. E. Lammert, and V. H. Crespi, Catalytic nanomotors: Autonomous movement of striped nanorods, *Journal of the American Chemical Society* **126**, 13424 (2004).
- [3] H. U. Bödeker, C. Beta, T. D. Frank, and E. Bodenschatz, Quantitative analysis of random ameboid motion, *EPL (Europhysics Letters)* **90**, 28005 (2010).
- [4] B. M. Friedrich and F. Jü, Chemotaxis of sperm cells (2007).
- [5] D. Selmeczi, L. Li, L. I. Pedersen, S. F. Nrrelykke, P. H. Hagedorn, S. Mosler, N. B. Larsen, E. C. Cox, and H. Flyvbjerg, Cell motility as random motion: A review (2008) pp. 1–15.
- [6] B. Nordén, Y. Zolotaryuk, P. L. Christiansen, and A. V. Zolotaryuk, Ratchet due to broken friction symmetry, *Physical Review E - Statistical Physics, Plasmas, Fluids, and Related Interdisciplinary Topics* **65**, 10.1103/PhysRevE.65.011110 (2002).
- [7] S. Denisov, Particle with internal dynamical asymmetry: chaotic self-propulsion and turning (2002).
- [8] S. Cilla, F. Falo, and L. M. Floría, Mirror symmetry breaking through an internal degree of freedom leading to directional motion, *Physical Review E - Statistical Physics, Plasmas, Fluids, and Related Interdisciplinary Topics* **63**, 10.1103/PhysRevE.63.031110 (2001).
- [9] E. L. Barnhart, G. M. Allen, F. Jülicher, and J. A. Theriot, Bipedal locomotion in crawling cells, *Biophysical Journal* **98**, 933 (2010).
- [10] P. Romanczuk, W. Ebeling, U. Erdmann, and L. Schimansky-Geier, Active particles with broken symmetry, *Chaos* **21**, 10.1063/1.3669493 (2011).
- [11] K. V. Kumar, S. Ramaswamy, and M. Rao, Active elastic dimers: Self-propulsion and current reversal on a featureless track, *Physical Review E - Statistical, Nonlinear, and Soft Matter Physics* **77**, 10.1103/PhysRevE.77.020102 (2008).
- [12] D. M. Fieguth, T. Schlachter, D. S. Brady, and J. R. Anglin, Hamiltonian active particles in an environment, *Phys. Rev. E* **106**, 044201 (2022).

- [13] L. Gilz, E. Thesing, and J. R. Anglin, Hamiltonian analogs of combustion engines: A systematic exception to adiabatic decoupling, *Phys. Rev. E* **94**, 042127 (2016).
- [14] A. I. Neishtadt, Probability phenomena due to separatrix crossing, *Chaos* **1**, 42 (1991).
- [15] A. I. Neishtadt, Averaging, passage through resonances, and capture into resonance in two-frequency systems, *Russian Mathematical Surveys* **69**, 771 (2014).
- [16] T. Eichmann, E. P. Thesing, and J. R. Anglin, Engineering separatrix volume as a control technique for dynamical transitions, *Physical Review E* **98**, 10.1103/PhysRevE.98.052216 (2018).
- [17] M. V. Smoluchowski, Drei Vortrage über Diffusion, Brownsche Bewegung und Koagulation von Kolloidteilchen, *Zeitschrift für Physik* **17**, 557 (1916).
- [18] H. Kramers, Brownian motion in a field of force and the diffusion model of chemical reactions, *Physica* **7**, 284 (1940).
- [19] M. Freidlin, Some remarks on the smoluchowski-kramers approximation (2004).
- [20] K. K. Sekimoto, *Stochastic energetics*, Lecture notes in physics, 799 (Springer, Berlin, 2010).